

## SURFACE PRESSURE DISTRIBUTIONS IN NORMAL TRIANGULAR TUBE ARRAYS

John Mahon, Julie Harel & Craig Meskell  
*Trinity College Dublin, Ireland*

### ABSTRACT

*Surface pressure measurements are presented for a cylinder in the third row of three normal triangular tube arrays ( $P/d=1.32$ ;  $1.58$ ;  $1.97$ ) with air cross flow. Surface pressure measurements were also made when the cylinder was statically displaced. Forces were calculated from the pressure measurements enabling an understanding of the force generation mechanism. The results show that the fluid force coefficients do not scale with the dynamic head but exhibit a dependency on Reynolds number and pitch ratio. However, no simple parameterisation was found for the lift force. Jet switching was found in  $P/d=1.58$  even when the tube was displaced. This phenomenon resulted in the large asymmetry observed in the pressure distribution around a static cylinder.*

### 1. INTRODUCTION

The mechanism responsible for fluidelastic instability (FEI) in tube arrays has been described by two theoretical frameworks: the “wavy-wall” model (Lever and Weaver (1986)); and the quasi-steady model (Price and Paidoussis (1984)). In addition, there have been a number of numerical simulations of FEI using Large Eddy Simulation, Reynolds Averaged Navier Stokes and vortex methods. However, the approach to validating all of these models depends primarily on comparison of predicted critical velocity to experimental values. Unfortunately, while this threshold is ultimately of greatest interest from a practical point of view, the experimental data available shows a significant scatter. In order to provide an initial validation database of the assumptions and predictions of these models, a detailed survey of the surface pressure distribution on a statically displaced cylinder in normal triangular tube arrays has been conducted. While there is already limited pressure data in the literature (Achenbach (1969), Zdravkovich and Namork (1980), Zukauskas et al (1983)), pressure distributions are available for only a few Reynolds numbers.

Furthermore, there appears to be no comprehensive studies of the pressure field around a statically displaced cylinder within a tube array available. Batham (1973) presented a limited study of the pressure distribution around a statically displaced cylinder in an array. The configuration used was a ten row in-line array with pitch ratio of 1.25. It was reported that the first three rows were displaced by 0.25mm which corresponds  $\sim 0.5\%$  tube displacement and that the pressure distribution “completely changed”. However no detailed results were presented.

### 2. EXPERIMENTAL SETUP

The experimental facility consists of a draw down wind tunnel with the tube array under investigation installed in the test section. The configurations under test were three five row normal triangular (NT) tube arrays with pitch ratios of 1.32, 1.58 and 1.97 with air cross flow. The flow velocity in the wind tunnel test section ranged from 2m/s to 18m/s with a free stream turbulence intensity of less than 1%. The tubes in the array are rigidly fixed, except for one tube which will be referred to as the instrumented cylinder.

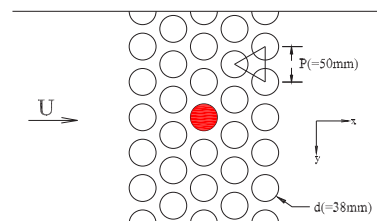


Figure 1:  $P/d=1.32$ ; Test section schematic

The instrumented cylinder has thirty six pressure taps at the mid-span around the circumference of the cylinder. The tube was mounted on a bidirectional traverse (located outside the wind tunnel) allowing a specific static displacement to be applied to the cylinder. Each tapping was monitored with a Senotec differential pressure transducer with the reference vented to at-

mosphere. In effect the gauge pressure was measured. The readings from the pressure transducers were digitised and logged using an NI 8 channel, 24 bit data acquisition frame. Each channel was simultaneously sampled and automatically low pass filtered to avoid aliasing.

### 3. RESULTS

#### 3.1. Validation of the test set up

In the first instance the experimental setup was validated by measuring the mean pressure distribution around an isolated cylinder and comparing the results with those in the literature. The measurements were acquired at a sample frequency of 64Hz and for 120 seconds. This low sample rate (dynamic range of 29Hz with anti-aliasing filters) removes any fluctuations due to vortex shedding. The pressure distribution was non-dimensionalised and the results presented in terms of the mean pressure coefficient. The pressure coefficient,  $C_P$ , was defined as

$$C_P = 1 - \frac{P_{\theta_{max}} - P_{\theta}}{\frac{1}{2}\rho U_g^2} \quad (1)$$

where  $P_{\theta_{max}}$  refers to the mean pressure at the stagnation point,  $P_{\theta}$  refers to the local mean static pressure at a given angular distance (also referred to as position angle) and is defined as the positive clockwise angle starting from the front of the cylinder (see Fig. 2),  $U_g$  is the gap velocity ( $U_g = U(\frac{P}{P-d})$ ) and  $\rho$  is the fluid density. The pressure coefficient was expressed in this way as taking the free stream static pressure as the reference pressure was not relevant as the mean static pressure varies throughout the array.

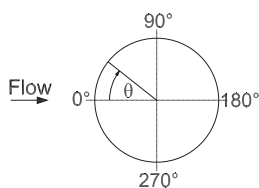


Figure 2: Schematic of position angle

The mean pressure coefficient at a Reynolds numbers of  $5.6 \times 10^4$  for an isolated cylinder is shown in Fig. 3. The curve compares well with data in the literature. However, small differences are observed which are attributed to the lower Reynolds number tested in this study. Also surface finish and flow conditions are reported to be important parameters for the location of the separation points which could contribute to the slight differences observed.

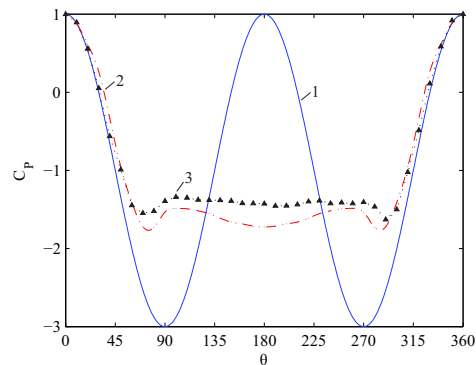


Figure 3: Distribution of pressure coefficient over the surface of a cylinder: 1) —, potential flow theory; 2) - · -, experimental data from the literature ( $Re = 8 \times 10^4$ ), Zukauskas (1989); 3) ▲, experimental data ( $Re = 5.6 \times 10^4$ ), current study

#### 3.2. Pressure Distribution

The pressure distributions around a cylinder in the third row in three arrays are presented for a range of Reynolds numbers ( $2 \times 10^4$  to  $1 \times 10^5$ ) and tube displacement ( $0 < y/d < 10\%$ ).  $C_P$  for all three arrays at  $y/d=0\%$  is shown in Fig. 4. For all three arrays the distribution is different to that observed for an isolated cylinder. It is also apparent that the neighbouring cylinders in the more compact array has a larger effect as shown by the deceleration of the fluid flowing through the inter-row gap. Examining the pressure distribution around the whole of cylinder reveals that there was slight asymmetry in the pressure distribution ( $P/d=1.32$ ). This was attributed to a rotational offset in the position angle. This resulted in a non zero lift force when the tube was un-displaced ( $y/d = 0\%$ ). However, the offset was quantified and accounted for in the calculation of the lift and drag forces. For  $P/d=1.58$  the distribution was not well behaved showing large asymmetry, in this case the large asymmetry was attributed to flow instability and will be discussed further below.  $P/d=1.97$  shows asymmetry resulting in a peculiar effect with the lift force which will be discussed later.

The effect of Reynolds number was also apparent in all three arrays. For  $P/d=1.32$  there was a Reynolds number dependency at lower Reynolds number. As the Reynolds numbers is increased  $C_P$  tends towards collapsing to a curve. For  $P/d=1.58$  the pressure distribution was found to be evolving at all Reynolds numbers tested. Its thought that the poorness of the relationship between pressure and dynamic head was augmented by the flow instability. For  $P/d=1.97$  there was a

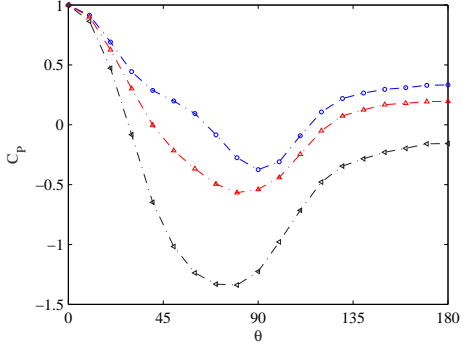


Figure 4:  $C_P$  comparison at the three pitch ratios tested:  $\circ$ ,  $P/d=1.32$ ,  $Re = 8.93 \times 10^4$ ;  $\triangle$ ,  $P/d=1.58$ ,  $Re = 8.77 \times 10^4$ ;  $\blacktriangle$ ,  $P/d=1.97$ ,  $Re = 8.69 \times 10^4$

Reynolds number dependency at lower Reynolds number. At higher Reynolds number the  $C_P$  collapses well.

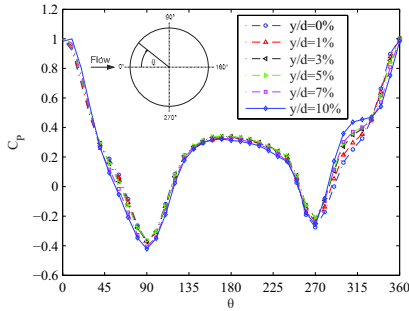


Figure 5:  $P/d=1.32$ ;  $C_P$  at various tube displacements,  $U = 7m/s$  ( $Re = 7.82 \times 10^4$ )

Displacing the tube resulted in the stagnation point moving in the direction opposite to the tube displacement and this occurred in all three arrays. The change in pressure distribution as a result of tube displacement became less pronounced with increasing pitch ratio. This is not surprising as the geometry was the most restrictive in the more compact arrays. The largest changes in pressure coefficient was observed in the region of the minimum gap between the cylinders both in the row ( $\theta = 90, 270^\circ$ ) and inter-row ( $\theta = 30, 330^\circ$ ) gaps as a result of a change in the flow velocity resulting from the change in blockage. For  $P/d=1.58$  the largest changes occurred at the minimum gap and to a lesser extent at the inter-row gap. Furthermore, in this array the occurrence of jet switching sometimes obscured the effect of the tube displacement as well as affecting the reference pressure used in  $C_P$ . Hence the actual pressure rather than the pressure coefficient is used to present the results for the pitch

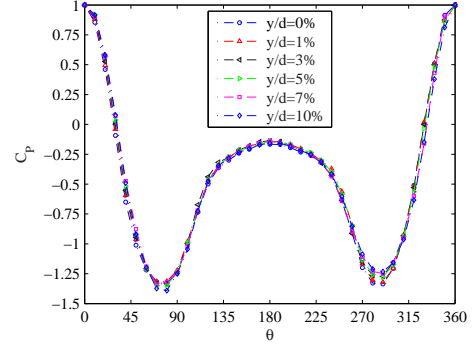


Figure 6:  $P/d=1.97$ ;  $C_P$  at various tube displacements,  $U = 18m/s$  ( $Re = 9.78 \times 10^4$ )

ratio of 1.58. As the pitch ratio was increased ( $P/d=1.97$ ) the effect of tube displacement was negligible. In fact, the largest change as a result of tube displacement occurred at the front of the cylinder and not at the minimum gap between neighbouring cylinders. This suggests that the effect of the neighbouring cylinders was very small especially as the largest changes resulted from the redistribution of the fluid impinging on the front of the cylinder.

As highlighted above, the mean pressure distribution for the pitch ratio of 1.58 showed significant asymmetry. When tests were repeated the pressure distribution changed (most noticeably in the region of the minimum gap between neighbouring cylinders) suggesting that the asymmetry distribution was due to flow instability. Similar observations have been reported previously in the literature. Further investigation demonstrates that flow instability was the cause. Examination of the raw pressure signals (Fig. 7), showed that there was significant variation in the pressure and at some positions where the asymmetry was more pronounced, there appeared to be a bi-stable flow regime (jet switching). Additional tests examining the local velocity field are also in agreement. In addition, some rudimentary flow visualisation was performed which further supports the findings from both the pressure and velocity data. The effect of the jet switching was also borne out in the lift force. Fig. 8 shows time resolved lift and drag force data at  $U=11m/s$  and  $y/d=0\%$ , a bi-modal characteristic was found for the lift force. However, this was not the case for the drag force which was only weakly affected by jet switching. This result is in agreement with the effect of local flow characteristics on the lift and drag force discussed below.

Most interestingly, the jet switching also occurred even when geometric symmetry was bro-

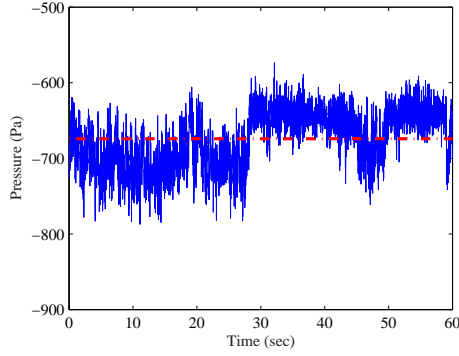


Figure 7: Pressure Signal;  $y/d=0\%$  at  $\theta=230^\circ$

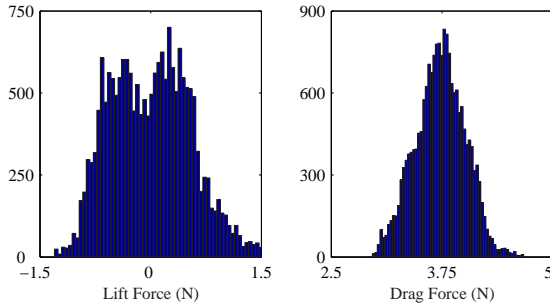


Figure 8: Histogram of time resolved lift and drag forces at  $U=11\text{m/s}$  and  $y/d=0\%$

ken (i.e. for non-zero tube displacement) and at all displacements ( $y/d=1-10\%$ ) tested. As jet switching was also observed at the largest displacement of  $y/d=10\%$ , this might suggest a strong coanda effect in the leeward cylinders although preliminary flow visualisation did not reveal anything to verify this possibility. It would also appear that the nature of the flow instability changes somewhat at the larger displacements. Examining the pressure distribution with the spread imposed shows that the spread was increased on the front face of the cylinder. Examination of the temporal pressure signal reveals bistable flow (jet switching) occurs in this region. As the nature of the fluid in a coanda effect is for the fluid to follow the curvature of the body the fluid is flowing around. It is not unreasonable to suggest that fluid was following the curvature of the leeward cylinders and detaching at some point. When the displacement was small the detached fluid impinges in the region  $40 - 70^\circ$  and  $290 - 320^\circ$  and as the displacement is increased this moves towards  $\theta = 350^\circ$ .

Fluid forces associated with fluidelastic instability are dependent on structural motion. Hence, fluid forces associated with fluidelastic instability on a rigid cylinder do not exist. How-

ever, it is possible to estimate the fluidelastic forces from static measurements made on a displaced body but it must be clear that this is not the same thing. This approach has been employed by many researchers in modelling fluidelastic instability (quasi-steady analysis). The fluid forces were obtained by decomposing the surface pressure distribution around the cylinder into the in flow drag force and the normal lift force components. The asymmetry due to rotation offset in the position angle as discussed above was quantified and accounted for when calculating the lift and drag forces ( $D = -\int_0^{2\pi} P d l \cos(\theta + \Delta\theta) d\theta$ ). The effect of a static tube displacement within a rigid array on the fluid forces is also discussed.

The drag force discussed herein is pressure drag as friction drag can be ignored for the Reynolds number range under test in this study. Fig. 9 plots the drag force against the gap velocity for  $P/d=1.32$ . Both scales are logarithmic. The data collapses well using a single line and drag force can be described using the following expression.

$$D = \frac{1}{2} \rho C_D l d U_g^n \quad (2)$$

Using linear regression, the resulting index,  $n$ , obtained was 1.68. This is different to the traditionally assumed value of 2 (scaling with dynamic head). When the tube was displaced the system behaved similarly with a line fitting the data sets. Fig. 10 plots the extracted indices against tube displacement. The index generally increases with tube displacement. The index changes from 1.68 at  $y/d=0\%$  to a maximum of 1.78 at  $y/d=10\%$  tube displacement. This corresponds to less than 6% variation in the index for the whole range of tube displacements. For the velocity range tested this resulted in a change in the drag force of 12% at most. This suggests that the drag force was only weakly affected by tube displacement.

For  $P/d=1.58$  the spread in the drag force increased and was attributed to the jet switching observed in this array. Increasing the duration of the tests and averaging the repeated tests reduced the spread in the data. Again, the drag force was plot against gap velocity with logarithmic axes. A single line did not fit the data well. A quadratic fit resulted in an improvement at lower Reynolds numbers but was poor at higher Reynolds numbers. In both fits the residuals forces were not random and appeared to take a periodic form illustrating the poor quality of the fits. The data collapsed well using two lines. In-

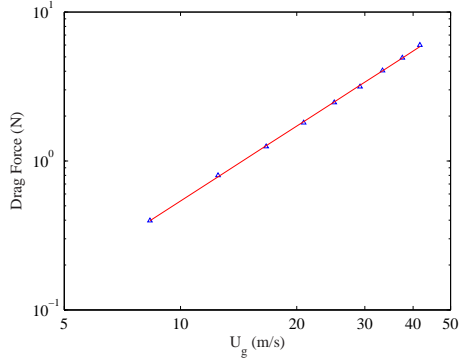


Figure 9:  $P/d=1.32$ ; Drag Force,  $y/d=0\%$

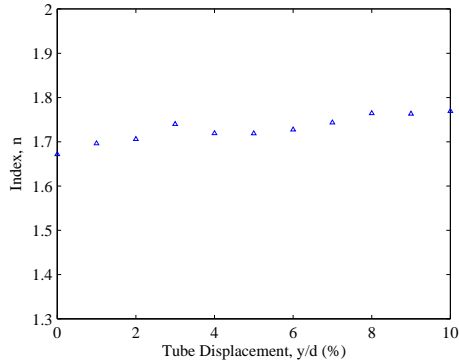


Figure 10:  $P/d=1.32$ ; Index relating drag force and gap velocity

indices of 1.4 and 2.3 were obtained for the lower and higher Reynolds numbers, respectively. The two lines suggest that there is a transition from one flow regime to another ( $Re \approx 6.6 \times 10^4$ ). This would be in agreement with the literature where it is reported that the critical region occurs at lower Reynolds number for tube arrays where the transition region is dependent on array geometry (isolated cylinder,  $Re \approx 2 \times 10^5$ ). When the tube was displaced the system behaved similarly with two lines collapsing the data. However, unlike  $P/d=1.32$  the indexes did not increase with tube displacement, they fluctuated about mean values which corresponded to 1.4 and 2.3 as shown in Fig. 11. For  $P/d=1.58$  the effect of tube displacement was smaller than the denser array. In addition the most significant changes arising in the pressure distribution from the tube displacement occur at the top and bottom of the cylinder where the contribution to the drag force was small. As it was observed that effect of tube displacement on the drag force was small, the drag force at all tube displacements was collapsed onto a single plot and was averaged (Fig. 12). The resultant indexes obtained

where 1.4 and 2.3 for lower and higher Reynolds numbers, respectively. A similar observation was observed for  $P/d=1.97$ . In fact the effect of tube displacement was smaller resulting in the drag force data at all tube displacements collapsing very well. The indices obtained were 1.4 and 2 for the lower and higher Reynolds numbers, respectively, with transition from one flow regime occurring at a slightly higher Reynolds number ( $\approx 6.8 \times 10^4$ ).

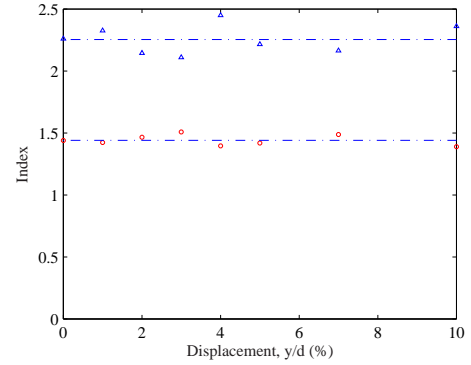


Figure 11:  $P/d=1.58$ ; Index relating drag force and gap velocity;  $\circ$ ,  $U_g < 24.5\text{m/s}$ ,  $Re < 6.6 \times 10^4$  and  $\Delta$ ,  $U_g > 24.5\text{m/s}$ ,  $Re > 6.6 \times 10^4$

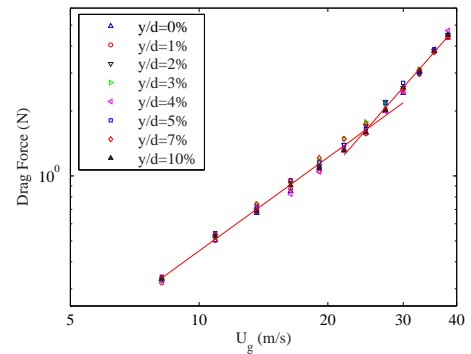


Figure 12:  $P/d=1.58$ ; Drag Force at all tube displacements with fitted lines

The lift force is given the same form as the drag force with the drag coefficient term,  $C_D$ , being replaced with the lift coefficient term,  $C_L$ . For  $P/d=1.32$  the lift force around a cylinder in an array appears to be very well behaved. When  $y/d = 0\%$  the lift force fluctuated around zero. When the tube was displaced, a net lift force in the direction opposite to the tube displacement results. The magnitude of the force generally increased with tube displacement and velocity.

Although the lift force was well behaved, increasing in magnitude with increasing displacement and velocity, no simple parameterisation

in terms of displacement and flow velocity was found. It was found that using  $L = \frac{1}{2}\rho C_L l d U_g^2$  was poor as the lift force was found not to scale with dynamic head. Normalising the lift force with respect to various different parameters did not collapse the data. This was because the lift force was far more susceptible to a change in displacement than the drag force. In fact, the lift force increases from  $\sim 0.5N$  to  $\sim 3N$ , when the tube was displaced from  $y/d = 1\%$  to  $y/d = 10\%$ . The upper value of the lift force approximately corresponds to  $\sim 40\%$  of the drag force for the same setup and conditions. Unlike, the drag coefficient, the lift force was not as dependent on the bulk pressure drop across the array but was influenced by the local flow characteristics.

The lift force in the pitch ratio of 1.58 was more complex than the pitch ratio 1.32 as a result of the flow instability. Again the lift force increased with tube displacement, however on some occasions the force increase was more significant and/or the force was in the opposite direction. Again no simple parameterisation was found.  $P/d=1.97$  shows asymmetry resulting in a peculiar effect with the lift force fluctuating about zero at lower Reynolds numbers and a net force generated at higher Reynolds numbers. This was not attributed to a rotational offset and can only be explained by a flow induced phenomena. Examining the raw pressure signal showed no flow instability. Flow visualisation was attempted to further understand the nature of the flow but proved to be unsuccessful. It was observed that different magnitudes of fluctuations were found on both sides of the cylinder suggesting differences in the wake of the leeward cylinder. However, further experiments are required to better understand the pitch ratio of 1.97.

It was reported above that the lift force did not scale with dynamic head for all arrays tested and that no simple parameterisation between lift force and velocity was obtained. In this instance as no simple parameterisation was found using  $C_L$  from  $L = \frac{1}{2}\rho C_L l d U_g^2$  can be used but it must be clear that it is a function of flow velocity, tube displacement and array geometry (including both array configuration and pitch).

#### 4. CONCLUSIONS

Some base line surface pressure measurements for a tube in the third row of three normal triangular tube arrays have been conducted with various static displacements applied to the tube. This data provides a valuable reference for val-

idation of simulations of FEI in staggered arrays. The flow structure in the pitch ratio of 1.58 was unstable and jet switching was observed even when geometric symmetry was broken.

The fluid forces did not scale with dynamic head as generally assumed by models in the literature. The drag force scaled with some other form of velocity which was dependent on array pitch and Reynolds number.

For  $P/d=1.32$  the lift force behaved well increasing with velocity and tube displacement. For  $P/d=1.58$  this well structured behaviour was interrupted by jet switching.  $P/d=1.97$  showed a peculiar lift distribution requiring further investigation. For all array pitches tested no simple parameterisation was found for the lift force as it was observed to be highly dependent on the flow velocity, array geometry and tube displacement.

#### 5. ACKNOWLEDGEMENTS

This publication has emanated from research conducted with the financial support of Science Foundation Ireland.

#### 6. REFERENCES

- Achenbach, E., 1969, Investigations on the Flow through a Staggered Tube Bundle at Reynolds Numbers up to  $Re = 10^7$ . *Warmddote und Stoffdotubertragung* **Bd 2**: 47-52.
- Batham, J. P., 1973, Pressure Distribution on in-line tube arrays in cross flow. *International Symposium, Vibration Problems in Industry, Keswick, U.K. Paper No. 411*: 1-24.
- Zdravkovich, M. M., Namork, J. E., 1980 Excitation, amplification and suppression of flow-induced vibration in heat exchangers *Proceedings Practical Experiences with Flow Induced Vibrations* 107-117.
- Zukauskas, A. A. et al, 1983, Heat transfer in Separated Flows at  $Re$  between 1 and  $2 \times 10^6$  and  $Pr$  between 0.7 and 10,000 (Separation of Vortices from Tubes). *Heat Transfer - Soviet Research* **15**(2): 73-80.
- Price, S. J., Paidoussis, M. P., 1984 An improved mathematical model for the stability of cylinder rows subject to cross-flow. *Journal of Sound and Vibration* **97** (4): 615-640.
- Lever, J., Weaver, D., 1986 On the stability of heat exchanger tube bundles. Part I: modified theoretical model. Part II: numerical results and comparison with experiment *Journal of Sound and Vibration* **107**: 375-410.
- Zukauskas, A. A., 1989, Cylinders in Crosflow, High-Performance Single-Phase Heat Exchangers. *Hemisphere Publishing Corporation* Chapter 10: 187-206.